Eurasian Chem.-Technol. J. 27 (2025) 71–88
The journal of the Institute of Combustion Problems https://ect-journal.kz

https://doi.org/10.18321/ectj1656

MXene-Based Electrocatalysts for Alkaline Water Electrolysis: a Review

M. Ryabicheva[1], Y. Zhigalenok[1], M. Skakov[2], Y. Koyanbayev[3], A. Miniyazov[3], F. Malchik[1,4]*

[1]Al-Farabi Kazakh National University, 71, al-Farabi ave., Almaty, Kazakhstan
[2]RSE "National Nuclear Center of the Republic of Kazakhstan", 2B, Beibyt atom str., Kurchatov, Kazakhstan
[3]Branch "Institute of Atomic Energy" of the RSE "National Nuclear Center of the Republic of Kazakhstan",
2B, Beibyt atom str., Kurchatov, Kazakhstan
[4]Center of Physical-Chemical Methods of Research and Analysis, al-Farabi Kazakh National University,
Tole bi str., 96A, Almaty, Kazakhstan

Article info

Received:
10 January 2025

Received in revised form:
18 February 2025

Accepted:
25 April 2025

Keywords:
Water electrolysis
Hydrogen evolution reaction
Alkaline electrolyte
Electrocatalyst
2D materials
MXene

Abstract

The growth in energy consumption and the limited nature of fossil resources are driving the search for alternative energy sources. Hydrogen is an environmentally friendly fuel, especially when produced by water electrolysis. However, its efficiency depends on the overpotential at the electrodes, which is related to the choice of catalyst. Noble metals, such as platinum, are effective but expensive. An alternative is catalysts based on transition metals, especially in alkaline media, where they are more resistant to corrosion. Oxides, nitrides, sulfides, and phosphides exhibit the highest catalytic activity; however, their efficiency is limited due to particle aggregation and poor adhesion to the substrate. MXene materials – layered transition metal carbides and nitrides – possess high electrical conductivity, stability, and potential for modification. They form robust freestanding electrodes, effectively bind with additives, and provide a large contact area with the electrolyte. This review analyzes hydrogen evolution reaction catalysts in alkaline media based on MXene and its modifications. Key relationships between the composition, structure, and activity of the catalysts are identified, and pathways to improve the quality of research in this field are proposed.

1. Introduction

In the modern world, there is a constant increase in energy consumption. Fossil fuels such as coal, oil, and gas serve as the primary energy sources. This leads to the gradual depletion of their reserves, and their combustion process contributes to atmospheric pollution with greenhouse gases [1]. These circumstances compel humanity to seek alternative energy sources, among which hydrogen is the most environmentally friendly. However, currently widespread methods for its production – coal gasification and steam methane reforming – are accompanied by carbon dioxide emissions and require high temperatures [2]. The most environmentally sound method for producing this fuel is water electrolysis, which involves two processes: hydrogen evolution at the cathode and oxygen evolution at the anode [3]. As water electrolysis is an energy-intensive process, primary energy consumption is related to electricity usage. To reduce this consumption, specifically the operating voltage of the process, catalysts are actively being developed for both electrode reactions – hydrogen and oxygen evolution.

In recent years, interest in developing efficient catalysts for electrochemical hydrogen production has significantly increased (Fig. 1, search keywords were "hydrogen evolution reaction", "catalyst, "alkaline"). Alongside noble metal-based materials [4–6], which have already established themselves as highly active but are too costly, numerous studies have been conducted using catalysts based on transition metals [7–10] and even non-metallic materials [11–13]. Besides cost, the chemical stability of materials in the electrolyte, whether acidic or alkaline, is also a critical factor. In acidic environments, the use

---

*Corresponding author.
E-mail address: frodo-007@mail.ru

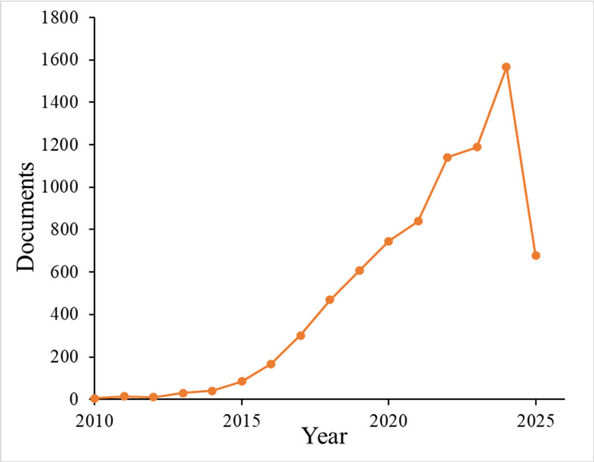

Fig. 1. Number of experimental articles on HER catalysts in alkaline media according to Scopus data (till May 2025).

of cheaper and sometimes more catalytically active non-noble materials is limited by their high susceptibility to corrosion, which reduces their lifespan. In alkaline electrolytes, however, transition metals and their compounds exhibit significantly less corrosion, making this medium more favorable for exploring new solutions in hydrogen production [14].

Various transition metal compounds, such as oxides, nitrides, sulfides, and phosphides, as well as non-metallic and hybrid catalysts combining different classes of compounds, are used as catalysts for the hydrogen evolution reaction (HER) in alkaline media [15]. Some of these materials exhibit high intrinsic catalytic activity, in some cases [7] achieving HER overpotentials even below 30 mV, which surpasses the performance of platinum. However, this high activity does not always translate into effective practical application due to the problem of nanoparticle agglomeration into larger clusters. Consequently, despite high intrinsic activity of the material, a substantial portion of it becomes inaccessible for the reaction, leading to inefficient utilization of expensive components and increased overall costs. To address the issue of low surface area, materials with a developed structure, such as nickel foam, are often used as substrates [8–10, 16]. Nevertheless, applying catalytic coating to such substrates presents another challenge: ensuring its stable adhesion to the metal surface is not always achievable [17], which, in turn, reduces the catalyst's durability.

Layered materials of the MXene class are transition metal carbides, nitrides, and carbonitrides, which can contain either a single type of transition metal [18–22] or a combination of them [23, 24]. The process of obtaining MXenes typically involves the synthesis of a so-called MAX phase (where M is a transition metal, A is a p-element such as Al, Si, etc., and X is carbon or nitrogen), which serves as a precursor. Subsequently, the A component is selectively etched from this MAX phase. This results in a suspension containing individual nanoscale layers (flakes) of MXene. Upon subsequent filtration of this suspension, the flakes self-assemble to form thin disks or films that are mechanically strong even without the use of a substrate or binders. It is important to note that this production method offers opportunities for easy material modification: for instance, various nanoparticles can be introduced into the MXene structure during the filtration stage to impart desired characteristics. This not only does not compromise the strength of the resulting MXene disks but, in some cases, can even further bind the individual layers together, enhancing the durability of the composite catalyst [25, 26]. Furthermore, MXenes possess a range of valuable properties: high electrical conductivity, large surface area, and the presence of various functional groups (-F, -Cl, -O, -OH) on their surface after etching, which facilitate the effective anchoring of diverse modifying additives [20, 27].

This review focuses on the analysis of MXene-based catalysts for the hydrogen evolution reaction in alkaline media. It covers pristine MXenes as well as their modified forms, including materials with altered surface groups, those doped with metal or non-metal atoms, and composites incorporating nanoparticles of various morphologies and chemical compositions. By comparing their characteristics, key correlations between the catalyst's composition/morphology and its efficiency are identified. Furthermore, the most promising materials based on their overall properties are determined, and avenues for the further improvement of research methodologies in this field are proposed.

2. Hydrogen evolution reaction, evaluated parameters, and catalyst requirements

During the electrolysis of aqueous solutions, the hydrogen evolution reaction occurs at the cathode [28]. The HER mechanism involves several sequential steps, as shown in Fig. 2, the specific pathway of which depends on the electrolyte's pH. The first step, known as the Volmer reaction, is the adsorption of a hydrogen atom onto the cathode surface. In acidic media, adsorbed hydrogen (H_{ads}) is formed through proton reduction, whereas in alkaline media, it arises from a water molecule with the simul-

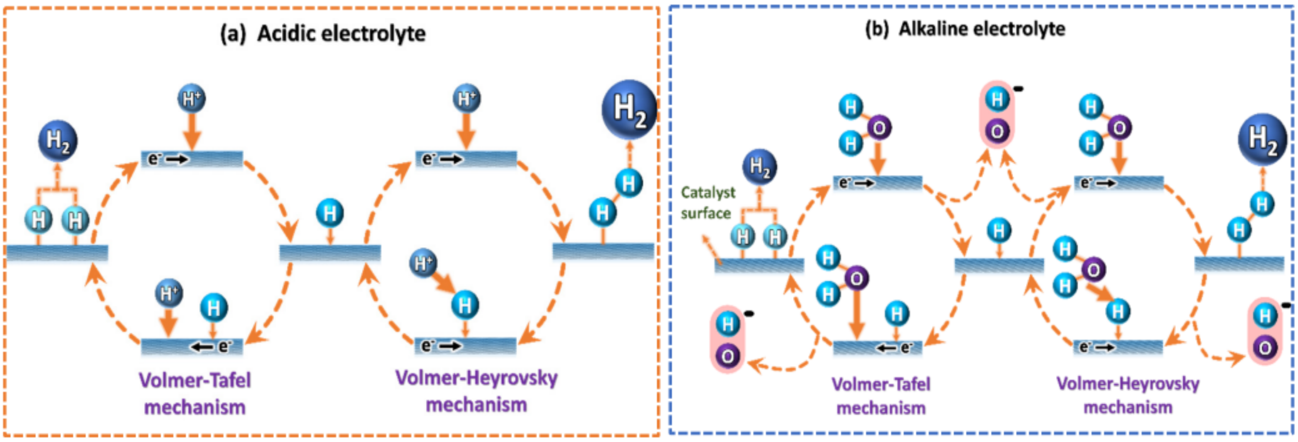

Fig. 2. Scheme of the HER mechanisms in (a) acidic and (b) alkaline media. Reproduced from Ref. [28]. Licensed under a Creative Commons Attribution (CC BY) license.

taneous release of a hydroxide ion. The subsequent formation of molecular hydrogen can proceed via one of two main pathways: the Heyrovsky reaction or the Tafel reaction. The Heyrovsky step involves electrochemical desorption, where a hydrogen molecule (H_2) is formed when an adsorbed hydrogen atom (H_{ads}) reacts with a proton (in acidic media) or with a water molecule (in alkaline media), accompanied by an electron transfer. Alternatively, the Tafel step is a chemical recombination: two hydrogen atoms (H_{ads}) adsorbed on the cathode surface combine to form an H_2 molecule, which then desorbs from the surface. It is important to note that the Tafel step, unlike the Heyrovsky reaction, proceeds identically in acidic and alkaline media.

The assessment of catalyst efficiency in the hydrogen evolution reaction requires consideration of a combination of thermodynamic and kinetic parameters, as well as operational characteristics. Thermodynamically, the minimum voltage required for the electrolytic decomposition of water into hydrogen and oxygen under standard conditions is 1.23 V [15]. However, in practice, a higher voltage is always necessary to carry out this process. This is due to the need to overcome the energy barriers of the reactions at the cathode (HER) and the anode (oxygen evolution reaction), which manifest as respective overpotentials, as well as ohmic losses within the electrolyzer components. In experimental studies, the overall energy efficiency of the system is often assessed by the overall water splitting voltage, measured in a two-electrode configuration.

One of the fundamental thermodynamic descriptors that allows for the prediction of the intrinsic activity of an HER catalyst is the Gibbs free energy of atomic hydrogen adsorption (ΔG_{H*}). This value, typically calculated using quantum chemistry modeling methods, characterizes the binding strength of the reaction intermediate – adsorbed hydrogen atom (H_{ads}) – to the catalyst surface. According to Sabatier's principle [29], optimal catalytic activity is achieved with moderate adsorbate binding: excessively strong binding hinders their subsequent removal from the surface (e.g., in the Heyrovsky or Tafel steps), while excessively weak binding impedes effective adsorption (Volmer step) [30]. Therefore, a ΔG_{H*} value close to zero is desirable, corresponding to an energetically favorable pathway for all stages of the catalytic cycle.

Due to the finite rate of any electrochemical process, achieving a significant HER rate requires applying a voltage to the cathode that exceeds its equilibrium potential. This difference is termed overpotential (η) and serves as the primary measure of a catalyst's kinetic efficiency: the lower the overpotential needed to achieve a specific current density, the higher the material's catalytic activity.

For a deeper understanding of HER kinetics, the exchange current density (i_0) and the Tafel slope (b) are analyzed. The exchange current density, defined as the current density at zero overpotential (i.e., under equilibrium conditions for the given electrode reaction), characterizes the intrinsic ability of the material to catalyze the reaction. The Tafel slope, obtained from the linear relationship between overpotential and the logarithm of current density ($\eta = a + b \log|i|$), reflects the sensitivity of the reaction rate to potential changes and provides insight into the HER mechanism and its rate-limiting step. The combination of these parameters (i_0 and Tafel slope) determines the magnitude of the overpotential under various conditions (applied current or voltage).

In scientific literature, the overpotential required to achieve a current density of 10 mA/cm^2 (η_{10}) is widely used as an indicative criterion for comparing the efficiency of different HER catalysts.

Beyond activity, catalyst stability is a key characteristic. The material's durability under electrolysis conditions determines its potential for practical use. Stability is investigated using various electrochemical methods: chronoamperometry, which records the change in current density over time at a constant potential; chronopotentiometry, where the change in potential is monitored at a constant current density (this method is often considered to most accurately reflect real operating conditions); and long-term potential cycling (e.g., 1000–5000 cycles) with monitoring of the retention of catalytic characteristics, particularly the overpotential at a given scan rate.

Finally, the cost of the catalyst is a significant factor, determined by the price of raw materials and the complexity of its production technology and directly influences economic feasibility of scaling up production. More detailed information on HER catalyst parameters, their theoretical foundations, and determination methods can be found in our recently published review [15].

Thus, an effective HER catalyst should possess low overpotential and a small Tafel slope, have a Gibbs free energy of hydrogen adsorption close to zero, exhibit high stability under operating conditions, and be economically viable.

3. MXene synthesis. MXenes as HER catalysts

Currently, the primary approaches to MXene synthesis are "top-down" and "bottom-up" technologies, which are discussed in detail in review [31]. Summarizing the information presented there, one can highlight the specific features and main methods for each approach.

The "top-down" approach involves obtaining MXenes through the chemical processing of pre-synthesized layered MAX phases. The most common method consists of selectively etching (removing) the A-layer from the MAX phase structure using various etchants, such as hydrofluoric acid, mixtures of fluorides and acids (e.g., LiF/HCl), as well as chlorides and sodium hydroxide. Less common are other variations of this approach, for instance, treatment in molten salts, which requires high temperatures and is therefore energy-intensive, or electrochemical etching, which often demonstrates insufficient efficiency, as indicated in the same review [31].

The alternative "bottom-up" approach involves the direct construction of the MXene structure from simpler precursors. Such methods include chemical vapor deposition, which can be carried out in one or two stages, synthesis on various substrates, and plasma-enhanced pulsed laser deposition. Common to these methods is the direct reaction of metals (or their compounds) with carbon or nitrogen sources (often, for example, methane) to form the target 2D structure. However, "bottom-up" methods have significant drawbacks: they typically require very high temperatures (often exceeding 1000 °C) and lead to the formation of MXenes with a very compact, densely packed layer structure [31]. This significantly reduces the material's specific surface area, limiting its utility as a high-porosity matrix for catalysts. Furthermore, the use of a simplified composition of starting reagents in these methods results in the formation of a smaller number of surface functional groups, which play a key role in anchoring modifying additives and in exhibiting catalytic activity [32]. Considering these factors, it becomes evident why, in the vast majority of experimental works aimed at synthesizing MXenes for catalytic applications, preference is given to the chemical etching of MAX phases [26, 33–37].

The presence of diverse surface functional groups on MXene flakes formed during their synthesis (primarily by etching methods), along with their unique 2D structure, has provided the basis for active investigation into their potential as catalysts for the hydrogen evolution reaction. The evaluation of MXene catalytic activity is conducted using both experimental methods [38–41] and theoretical approaches, particularly quantum-chemical calculations [42, 43]. Computational methods offer valuable advantages, such as saving time and material resources. However, when modeling complex real-world electrochemical systems (including the electrolyzer, electrolyte, and electrodes), it becomes challenging to accurately account for the entire multitude of factors influencing the process, and some of these aspects are difficult or even impossible to adequately reproduce in theoretical models. Nevertheless, the Gibbs free energy of hydrogen adsorption is one of the key parameters frequently determined and widely used in theoretical studies to predict and compare the catalytic activity of various materials.

In addition to predicting ΔG_{H^*}, studies dedicated to the computational screening of various MXenes for their HER catalytic activity attempt to consider more complex aspects, such as the surface heterogeneity characteristic of experimentally synthesized samples. An example of such an approach is the research presented in reference [42]. The authors of this work selected 12 transition metals (Sc, Ti, V, Cr, Mn, Y, Zr, Nb, Mo, Hf, Ta, and W) from which MXene structures could potentially be formed. For these metals, the heats of formation of their corresponding carbides and nitrides were calculated, considering both unfunctionalized (pristine) MXenes and structures with different surface groups: -O, -OH, and -F. The calculation results indicated that MXenes terminated with oxygen (-O) or hydroxyl (-OH) groups are energetically more favorable, while compounds with fluorine (-F) groups and pristine MXenes were found to be thermodynamically less stable. Based on the conclusion of the thermodynamic preference for oxygen-terminated MXenes ($M_xC_yO_2$ or $M_xN_yO_2$), the authors proceeded to calculate the Gibbs free energy of hydrogen adsorption (ΔG_{H*}) for a wide range of such O-terminated MXenes, including combinations of two, three, and four different metals in their structure. From these calculations, the most promising compositions in terms of catalytic activity were identified as those for which the ΔG_{H*} value did not exceed 0.1 eV. These materials, listed in increasing order of their absolute $|\Delta G_{H*}|$ values, include (Fig. 3): Sc_2CO_2, $Cr_4C_3O_2$, $Mn_4C_3O_2$, $Y_4C_3O_2$, $Cr_4N_3O_2$, $V_3C_2O_2$, Cr_2CO_2, Cr_2NO_2, $Sc_4C_3O_2$, $Mn_4N_3O_2$, and Nb_2NO_2.

Furthermore, the values for another 9 variants did not exceed 0.2 eV, which corresponded to the threshold established in another similar study [43]. Since it was conducted later, it immediately considered only MXenes with oxygen surface groups. Also, only carbides were considered, and the selected list of metals coincided with the previous work, with the exception of yttrium, likely due to the complexity of synthesis or the high cost of reagents. The ΔG_{H*} values were calculated at low hydrogen atom coverage of the catalyst surface (1/18 H), whereas in study [42] this parameter varied between 25–100%, corresponding to the equilibrium state of the system; therefore, the Gibbs energies in these studies differed for the same structures. Within the established limit, MXenes with compositions Ti_2CO_2, Nb_2CO_2, $Zr_3C_2O_2$, and $W_{n+1}CnO_2$ [43] were found.

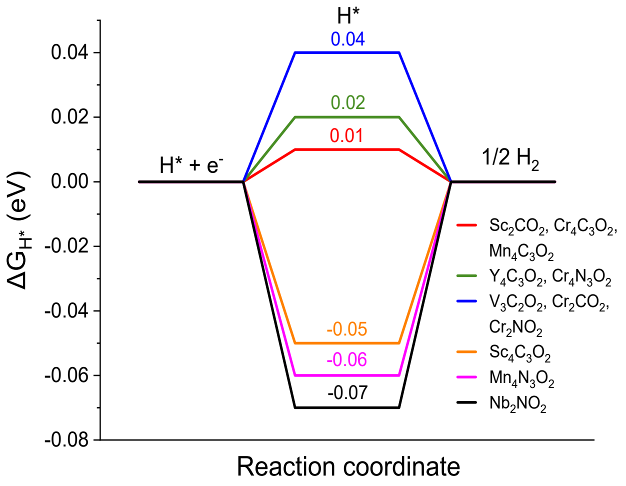

Fig. 3. ΔG_{H*} values for various MXenes based on theoretical calculations from reference [42].

Despite excellent calculated ΔG_{H*} values for individual MXenes, the expected low HER overpotentials were not achieved in practice; moreover, the aforementioned MXenes are almost not found in experimental studies, which is most likely due to their instability or complexity of synthesis. The most common MXene, $Ti_3C_2T_x$, depending on the synthesis pathway, exhibits an HER overpotential ranging from 610 to 740 mV in an alkaline medium [44]. Among other MXene compositions, the overpotential at 10 mA/cm^2 is 398 mV for $Nb_4C_3T_x$ [45], 570 mV for Ti_3CN [39], 376 mV for Mo_2CT_x [40], 516.4 mV for $Ti_{2.5}Nb_{0.5}C_2T_x$ [24], 271 mV for Ti_2NT_x [46], 315 mV for MoN [47], and for V_2CT_x it is 493 mV at 1.5 mA/cm^2 [48]. All these indicators are too high for the possibility of using MXenes in their pure form as HER catalysts, which indicates the necessity of their modification to enhance catalytic activity.

4. Application of MXenes with various additives as HER catalysts

4.1. Modification of MXenes by altering surface functional groups

Replacing the initial, often compositionally heterogeneous, surface groups of MXenes with specific functional groups of a single type represent the most technically straightforward and least resource-intensive modification method (Fig. 4). Such changes are typically achieved either by varying the conditions during the MAX phase etching stage or through post-treatment of the already formed MXene electrode. However, there is a limited number of studies in scientific literature dedicated to this type of MXene modification for producing hydrogen evolution reaction catalysts specifically in alkaline solutions. This might indirectly suggest a low efficiency of MXenes with surface groups modified in this manner in this particular medium.

Furthermore, the feasibility of using certain types of surface functional groups is questioned even at the theoretical calculation stage. For instance, an analysis of Pourbaix diagrams constructed for MXenes with various surface terminations has

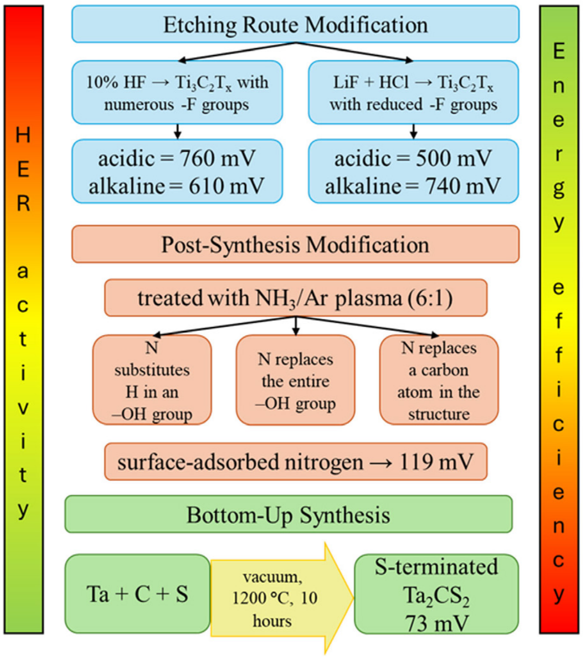

Fig. 4. Schematic illustration of MXene surface modification pathways for HER catalysis.

shown that the existence of fully H-terminated (hydrogen-terminated) MXene is possible only at very negative potentials relative to the reversible hydrogen electrode (RHE). Such a condition precludes its practical application as an HER catalyst [49].

Two main etching solutions are predominantly used to obtain the most common MXene, $Ti_3C_2T_x$, from the corresponding MAX phase: one based on hydrofluoric acid (HF) and another based on a mixture of lithium fluoride and hydrochloric acid (LiF-HCl). In many publications, the choice of a specific etchant is not always thoroughly justified [18, 26, 34, 36, 37, 50–54], possibly due to an assumption of their equivalence for the MXene formation process. However, a study [44] revealed that using the LiF-HCl solution results in the formation of considerably fewer fluorine-containing functional groups on the surface of $Ti_3C_2T_x$ flakes. This positively affects its catalytic activity in the hydrogen evolution reaction in acidic media: the overpotential was 500 mV at 10 mA/cm^2, whereas after etching in 10% HF, it reached 760 mV. In alkaline media, conversely, an opposite trend was observed: the catalyst obtained by HF etching showed a lower overpotential (610 mV) compared to the sample synthesized using LiF-HCl (740 mV) at the same current density. The authors attributed this to a reduction in fluorine content on the MXene surface directly in the electrolyte (in situ) in the former case, and to an initially lower fluorine content on the surface even before the electrochemical measurements in the latter.

Significantly better catalytic characteristics were achieved by modifying already exfoliated $Ti_3C_2T_x$ with nitrogen atoms [18]. For this, an MXene suspension, pre-intercalated with ammonium bicarbonate, was treated with an NH_3/Ar plasma mixture. Although the nitrogen dopant atoms were present in the resulting catalysts in three different forms (adsorbed on the surface replacing hydrogen in an OH group, replacing the entire OH group, and substituting a carbon atom in the MXene lattice), their ratio varied depending on the plasma composition. X-ray photoelectron spectroscopy results and theoretical calculations showed that the material with a predominance of surface-adsorbed nitrogen possessed the highest catalytic activity. Such material was obtained at an NH_3:Ar plasma ratio of 6:1. Electrochemical tests confirmed these findings: the overpotential of this catalyst at a current density of 10 mA/cm^2 was only 119 mV.

A completely different approach was used to synthesize an MXene with the composition Ta_2CS_2, containing exclusively sulfur atoms on the flake surfaces [55]. This material was obtained by direct synthesis from elemental tantalum, carbon, and sulfur via high-temperature annealing (1200 °C) in a vacuum for 10 hours. The resulting Ta_2CS_2 catalyst demonstrated an HER overpotential of 73 mV at 10 mA/cm^2, which is almost half that of commercial $Ta_4C_3T_x$ MXene (139 mV). However, when considering the practical applicability of this method, its high energy consumption is a key factor.

Thus, as anticipated, attempts to improve the catalytic properties of MXenes for HER in alkaline solutions by modifying their surface functional groups are either relatively ineffective [44] or require technically complex [18] or highly energy-intensive [55] methods.

4.2. Modification of MXenes with single metal atoms

One promising approach to modifying MXenes to enhance their catalytic activity in HER is the anchoring of single metal atoms, both noble and transition metals, onto their surfaces (Fig. 5). The use of noble metals in such a highly dispersed form allows for a significant reduction in the overall catalyst cost due to the lower consumption of the expensive component, while often maintaining high catalytic activity comparable to their bulk counterparts. Modification of MXenes with single transition metal atoms also leads to catalysts with respectable performance, which, moreover, can surpass the activity of the corresponding transition metals in their pure form [4].

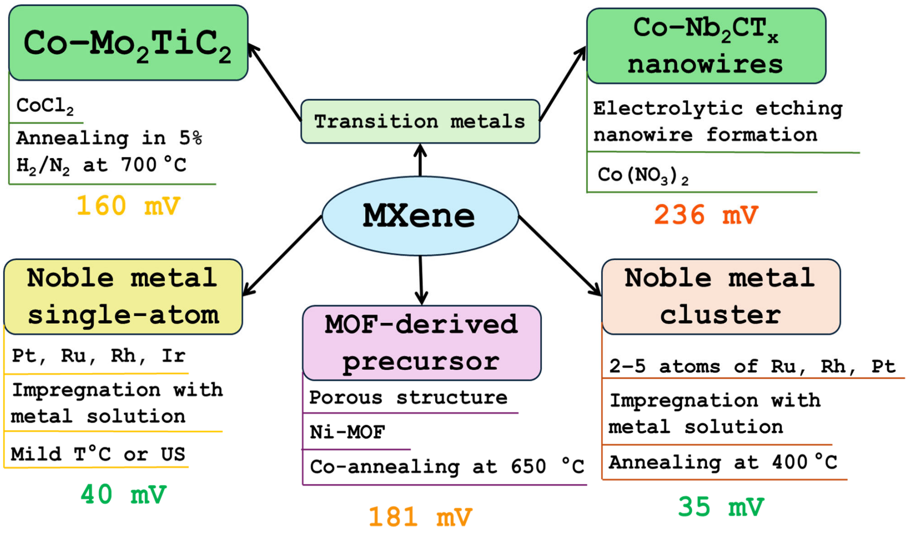

Fig. 5. Schematic illustration of MXene modification by metal single atoms for enhanced HER.

The standard synthesis method for such composite catalysts typically involves mixing an MXene suspension with a salt solution of the chosen metal [56]. Subsequent reduction of metal ions to their atomic state occurs directly on the surface of the MXene flakes, facilitated by oxygen-containing functional groups that act as nucleation and anchoring sites. This process can be carried out either at room temperature or with the application of thermal treatment (annealing) after mixing the components to ensure more effective metal reduction from the salt.

Despite the apparent energy advantage of MXene modification methods that do not require heating, the significant time investment they entail can reduce the overall practical efficiency. For instance, in study [57], single ruthenium atoms were successfully anchored onto $Ti_3C_2T_x$ MXene by impregnating the MXene suspension with a $RuCl_3$ solution for 18 h under constant stirring, without any additional intensifying treatments. Extended X-ray Absorption Fine Structure (EXAFS) data confirmed that ruthenium was attached to the MXene surface via Ru-O bonds, and the absence of peaks characteristic of Ru-Ru bonds indicated the formation of single atomic centers rather than metal nanoparticles. Although the low HER overpotential achieved in this case (40.3 mV at 10 mA/cm^2 and 464.6 mV at 1.5 A/cm^2) somewhat justifies the lengthy synthesis, it is likely possible to shorten the process by employing ultrasonic treatment or moderate heating.

On the other hand, the formation of small atomic clusters, rather than individual single atoms, can also lead to enhanced catalytic activity. For example, study [58] demonstrated that ruthenium clusters formed on titanium cluster vacancies within the $Ti_3C_2T_x$ crystal lattice exhibit higher efficiency compared to ruthenium anchored via oxygen bonds or on single vacancies. The HER overpotential for such a catalyst was 35 mV at 10 mA/cm^2, slightly lower than for the system with single Ru atoms [57]. The modification process itself took 14 h, of which 12 h were for drying the reactant mixture at 60 °C and only 2 h for annealing at 400 °C. In the same work, analogous catalysts with rhodium, platinum, and iridium clusters were also prepared and investigated; however, their HER catalytic activity was found to be lower compared to the MXene-ruthenium composite.

Despite the fact that transition metals generally possess lower intrinsic catalytic activity compared to noble metals, their use for modifying MXenes also allows for the creation of materials with noteworthy characteristics. For instance, the modification of Mo_2TiC_2 MXene with cobalt, carried out by treatment with cobalt chloride followed by annealing in a reducing atmosphere (5% H_2/N_2) in a tube furnace at 700 °C [23], led to an interesting catalyst. Although its activity at a standard current density of 10 mA/cm^2 was not very high (160 mV overpotential), at a significantly higher current density (400 mA/cm^2), the overpotential increased to only 321 mV. This value was even lower than that of a commercial Pt/C catalyst (366 mV) under the same conditions, indicating the promise of such an approach for operation under high current load regimes. In another example [19], Nb_2CT_x MXene was obtained in the form of nanowires using an electrochemical etching method. The resulting nanowires were further modified with cobalt ions by mixing the MXene suspension with a cobalt nitrate solution. X-ray diffraction analysis confirmed the presence of chemical bonds between cobalt atoms and the oxygen of MXene's surface functional groups. However, despite the synergistic effect from cobalt modification and the unique nanowire morphology, the resulting catalyst exhibited the highest catalytic activity only in comparison with other materials described in that same study. The recorded HER overpotential was 236 mV at 10 mA/cm^2, which is still substantially higher than that of several other catalysts modified with single metal atoms (especially noble metals). Nickel has also been used as a modifying transition metal. Modified Ni-$Ti_3C_2T_x$ was obtained by co-annealing $Ti_3C_2T_x$ with a nickel-based metal-organic framework (Ni-MOF) [59]. This procedure led to the formation of a catalyst with high porosity, which contributed to improved kinetics for the hydrogen evolution reaction.

Summarizing the discussed examples of HER catalysts based on MXenes modified with single metal atoms, it can be concluded that the best catalytic characteristics are achieved when using noble metals (that is economically justified at their low content as single atoms or clusters), or when using MXenes that inherently have a mixed transition metal composition in their structure.

4.3. Modification of MXenes with metal nanoparticles

An effective approach to creating highly active HER catalyst at relatively low cost is the modification of catalytically less active matrices with metal nanoparticles that possess high intrinsic catalytic activity (Fig. 6). The use of layered materials, such as MXenes, as support for such nanoparticles further helps to increase the catalyst-electrolyte contact area, which positively affects the overall process efficiency. For example, a catalyst created by growing platinum nanoparticles of quantum dot size (approximately 1.15 nm) on the surface of Nb_2CT_x nanowires at a relatively low temperature (150 °C) demonstrated an HER overpotential of only 65 mV at a current density of 10 mA/cm^2 [20]. This value was even lower than that of a bulk platinum plate (141 mV) tested in the same study. For composites of platinum with $Ti_3C_2T_x$ MXene, an optimal metal nanoparticle content of 2.4% was also determined [60]. At this concentration, their uniform distribution was achieved in a multi-level bulk structure obtained from a $Ti_3C_2T_x$ suspension by spray drying, which ensured exceptionally high HER activity with an overpotential η_{10} = 27 mV. Using a smaller amount of platinum (0.8%) led to decreased activity due to an insufficient number of active sites, whereas increasing the content to 4.2% caused the formation of platinum particles four times larger in size and, consequently, reduced the utilization efficiency of the expensive noble metal.

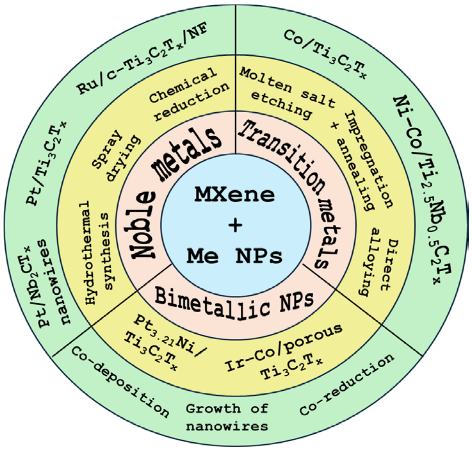

Fig. 6. Modification pathways of MXenes with metal nanoparticles for HER catalysis.

The hydrophilicity and aerophobicity of the catalyst surface play a significant role in HER, as improved electrolyte wettability and facilitated hydrogen bubble detachment promote mass transport. MXenes, due to the presence of oxygen-containing functional groups on their surface, exhibit favorable characteristics in this regard: as shown in study [61], the contact angles for a water droplet and an underwater hydrogen bubble were <15° and 168°, respectively. Nevertheless, the main enhancement in chemical catalytic activity in that particular study was achieved by incorporating ruthenium nanoparticles via hydrothermal synthesis. The modified Ru/c-$Ti_3C_2T_x$/NF catalyst (where NF is nickel foam) showed an HER overpotential of 37 mV at 10 mA/cm^2, whereas for the initial c-$Ti_3C_2T_x$/NF sample, it was 144 mV. Notably, good results can also be achieved with lower energy input during synthesis. For instance, Ti_3CN MXene modified with ruthenium nanoparticles through simple chemical reduction of $RuCl_3$ in the presence of sodium borohydride ($NaBH_4$) at room temperature demonstrated quite high HER efficiency with an overpotential of 56 mV at the same current density [39]. Slightly lower activity was shown by a catalyst based on Mo_2CT_x with relatively large ruthenium clusters (average size 50 nm), composed of 5-nanometer granules, anchored on its flakes [40]. The HER overpotential for this material was 78 mV, which is in good agreement with the previously noted trend in study [60]: an increase in nanoparticle size leads to some reduction in catalytic efficiency.

Transition metal nanoparticles have also been actively investigated as catalytically active additives for MXene modification. For example, etching the MAX phase Ti_3AlC_2 in molten cobalt chloride at 750 °C led to the simultaneous formation of MXene and the reduction of cobalt, which was distributed both in the interlayer space and on the material's surface [62]. Subsequent 12-hour treatment with a 0.5 M H_2SO_4 solution resulted in the removal of some surface cobalt, which enriched the MXene surface with oxygen-containing functional groups. This, in turn, further lowered the hydrogen evolution reaction overpotential on the resulting $Ti_3C_2T_x$:Co composite – values at 10 mA/cm^2 were 103.6 mV for the acid-treated sample and 150.3 mV for the sample without such treatment. Another example of an effective catalyst based on MXene modified with transition metal nanoparticles is $Ti_{2.5}Nb_{0.5}C_2T_x$ (an MXene with a mixed transition metal composition in its structure), the surface of which was modified with nickel-cobalt alloy nanodots with an average diameter of 5 nm [24]. This catalyst demonstrated a low HER overpotential – only 43.4 mV at 10 mA/cm^2. This result, as well as the previously mentioned good performance of the Co/Mo_2TiC_2 catalyst [23], may indicate a certain advantage in using MXenes that inherently contain several transition metals in their structure for creating highly active catalytic systems.

The combination of two different metals (e.g., a noble and a transition metal) within nanoparticles for MXene modification has also been considered a promising approach [27, 63]. However, an analysis of specific experimental data reveals certain problems and limitations of this direction. For instance, $Pt_{3.21}Ni$ nanowires anchored on $Ti_3C_2T_x$ flakes showed the lowest calculated hydrogen adsorption energy (ΔG_{H*}) compared to other Pt-Ni composites with different metal ratios, as well as compared to a commercial Pt/C catalyst (although the maximum difference in ΔG_{H*} was only about 0.1 eV). The measured HER overpotential on $Pt_{3.21}Ni/Ti_3C_2T_x$ at a current density of 5 mA/cm^2 was 56 mV (which extrapolates to 103 mV at 10 mA/cm^2) [63]. However, this catalyst exhibited extremely low stability in alkaline media: after only 2 h of operation, the current density dropped to 27% of its initial value. The authors attributed this to the blocking of MXene active sites by hydroxyl groups, which was confirmed by the disappearance of the fluorine (F) signal in XPS spectra after the stability test. This latter observation was noted as rather strange, considering the previously established negative impact of surface fluorine on the HER catalytic activity of MXenes [44]. Nanoparticles of another bimetallic composition, iridium-cobalt, in combination with porous $Ti_3C_2T_x$, also failed to show high catalytic activity: the HER overpotential on this composite at 10 mA/cm^2 was 135 mV [27].

Thus, the analysis shows that MXene modification with metal nanoparticles is most effective when using monometallic nanoparticles of elements that possess high intrinsic HER catalytic activity, particularly platinum and ruthenium. The use of nanoparticles of individual transition metals as modifiers can also be quite effective. However, in the examples discussed, the use of bimetallic nanoparticles (a mixture of a transition and a noble metal) did not lead to a significant synergistic increase in catalytic activity.

4.4. Modification of MXenes with nanoparticles of various compounds

The use of nanoparticles of various compositions and shapes as modifying additives to MXenes is primarily aimed at increasing the active surface area of these additives, which can contribute to improving the composite's catalytic properties (Fig. 7). The intrinsic catalytic activity of the resulting composites depends on the activity of the incorporated additives, which is often qualitatively assessed by the calculated Gibbs free energy of hydrogen adsorption (ΔG_{H*}). However, overall efficiency is also influenced by factors such as the often insufficient mechanical and chemical stability of catalysts under electrolysis conditions, as well as the size of the modifying nanoparticles themselves, which directly affects their contact area with the electrolyte. A significant problem when analyzing literature data is that information on both indicators is not provided in all studies.

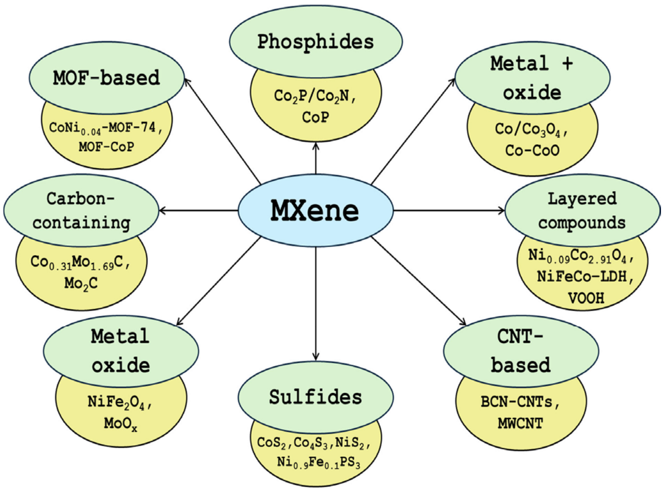

Fig. 7. MXene surface modification strategies with nanomaterials for enhanced HER catalysis.

Modification of MXenes with phosphorus compounds is most often carried out by introducing cobalt phosphide nanoparticles, although the catalytic activity of the resulting composites can vary significantly. For example, for $Ti_3C_2T_x$ MXene, obtained in a bulk structure to prevent the aggregation of individual flakes, cobalt phosphide (CoP) was formed on its surface by phosphidizing the corresponding oxide. The CoP particle size, according to transmission electron microscopy data, was in the range of 3–5 nm [64]. Electrochemical tests of this composite revealed a relatively high HER overpotential of 168 mV. For comparison, in study [65] for a CoP/Mo_2CT_x catalyst, where cobalt phosphide was present as nanowires, the HER overpotential was reduced to 78 mV, which the authors attributed specifically to the increased surface area of the active additive (CoP nanowires). Although one might also assume a contribution from the different MXene matrix composition ($Ti_3C_2T_x$ versus Mo_2CT_x, for which ΔG_{H^*} were -1.01 eV and 0.71 eV, respectively), the difference in ΔG_{H^*} for the additives themselves was more substantial (0.81 eV for pure phosphorus and only -0.079 eV for CoP), indicating a dominant role of the nature and morphology of the phosphide additive in these catalysts, rather than the MXene type. An exceptionally low HER overpotential (15 mV at 10 mA/cm^2) was achieved using a Co_2P/Co_2N modifier with a hierarchical structure (Co_2P particles coated with Co_2N nanoparticles) in combination with $Ti_3C_2T_x$ supported on nickel foam [50]. It is most likely that such outstanding activity was due precisely to the composite's architecture, which provided a very high specific surface area, as the calculated ΔG_{H^*} for this catalyst (0.105 eV) was noticeably higher (less optimal) than in other mentioned examples with cobalt phosphides.

Metal-Organic Frameworks are coordination polymers consisting of metal ions linked by organic ligands. Due to their high porosity and wide possibilities for varying chemical composition, MOFs are promising precursors for the synthesis of various catalytic materials. An interesting approach to modifying MXenes with phosphides involves coating MOF-derived phosphide crystals with MXene. The purpose of such a coating is to increase the electrical conductivity of the phosphide component, which, in turn, should lead to an increase in the overall catalytic activity of the composite. This method was implemented in study [46] for the synthesis of a Ti_2NT_x@MOF-CoP catalyst. The process involved the self-assembly of Ti_2NT_x MXene with a MOF precursor (ZIF-67), followed by decarbonization and phosphorization to convert ZIF-67 into CoP. The MOF-CoP material itself demonstrated good catalytic activity, judging by the slight difference in HER overpotentials for MOF-CoP (153 mV) and the Ti_2NT_x@MOF-CoP composite (112 mV), especially when compared to pristine Ti_2NT_x (271 mV). The large particle size of MOF-CoP (466 nm) also suggests that its intrinsic activity played a key role.

Furthermore, in another example [66], a MOF was used directly as a catalytically active additive to MXene. Hexagonal crystals of $CoNi_{0.04}$-MOF-74 with a significant average diameter (about 10 μm) were perpendicularly anchored on the surface of MXene, which, in turn, was deposited on nickel foam (NF) serving as a high-surface-area substrate. Despite the large MOF particle size, this composite achieved an HER overpotential of 102 mV at 10 mA/cm^2. This result is attributed to both the catalytic activity of the MOF itself and the increased overall surface area of the catalyst. For comparison, Ni-unmodified Co-MOF-74 on MXene/NF, as well as $CoNi_{0.04}$-MOF-74/NF and pristine MXene/NF individually, showed poorer results (overpotentials of 175, 203, and 217 mV, respectively). However, it is important to note that not all MOFs possess sufficient catalytic activity for HER. For instance, ZIF-8 material, as spherical particles with a diameter of 500 nm, exhibited a high HER overpotential (542 mV at 10 mA/cm^2) in its pure form, which was even higher than that of the MXene used (514 mV). Their composite only slightly reduced this value (to 502 mV), which is insufficient for creating a competitive catalyst [34].

Transition metal carbides are also used as modifying additives to MXenes, particularly $Ti_3C_2T_x$, although the catalytic activity of the resulting composites varies widely. For example, molybdenum carbide (Mo_2C) only reduced the HER overpotential to 219 mV at 10 mA/cm^2, despite additional improvements such as modifying these nanoparticles with phosphorus and coating them with N-doped carbon shells (obtained by pyrrole polymerization followed by annealing) [67]. Much better results were shown by a composite with a mixed carbide, $Co_{0.31}Mo_{1.69}C$, also protected by a graphene carbon shell – the overpotential in this case was already 75 mV at the same current density [68]. In this work [68], hydrogen adsorption energies were also calculated for carbides of different compositions; the minimum ΔG_{H^*} value (0.05 eV), most favorable for HER, was obtained for the graphene-coated $Co_{0.31}Mo_{1.69}C$, while for uncoated Mo_2C, it was -0.92 eV, which explains the lower activity of the catalyst in study [67].

Carbon-containing modifiers also include cobalt oxalate, which, with MXene, forms self-assembling nanotubes, allowing for a large contact area with the electrolyte; the ΔG_{H*} for such a composite is -0.16 eV [69]. The initial HER overpotential at a current density of 10 mA/cm^2 was 74 mV; however, after 5 successive linear voltammetry scans in 1M KOH, the value decreased to 28 mV due to the transformation of cobalt oxalate into its hydroxide, the latter forming as hexagonal plates perpendicularly attached to the nanotube surfaces. Most likely, it was this additional increase in surface area that enhanced the catalyst's efficiency, as the Gibbs free energy ΔG_{H*} shifted closer to zero by only 0.04 eV, albeit with the opposite sign (0.12 eV).

Interesting synergistic effects are also observed when modifying $Ti_3C_2T_x$ MXene with a mixture of a transition metal and its oxide, using cobalt as an example. On one hand, a comparison of hydrogen adsorption energy values for different active sites shows more favorable ΔG_{H*} values for HER on unoxidized metal [51]. On the other hand, a significant reduction in the overpotential for this process is observed on the mixed catalyst (87 mV) compared to the pure metal (443 mV) [70]. Different cobalt oxides are formed in the considered studies (CoO [51] and Co_3O_4 [70]), but a general difference in the contribution of the metal and oxide phases to the reaction catalysis can be assumed. In the case of a Co-CoO mixture, the calculated ΔG_{H*} values are closest to zero on the Co_0 active center, both with and without a $Ti_3C_2T_x$ matrix (0.232 eV and 0.271 eV, respectively). Meanwhile, on the oxidized cobalt Co^{2+} center, the adsorption energy is noticeably higher – 0.444 and 0.403 eV with and without MXene, respectively, indicating better hydrogen adsorption on pure cobalt. In the case of Co/Co_3O_4, it is stated that water molecule splitting occurs due to Co_3O_4, while the metal only improves the transport of adsorbed hydrogen atoms to each other to form hydrogen molecules. The surface area factor is also present: from the morphology schemes of $Co\text{-}CoO/Ti_3C_2T_x$ and $Co/Co_3O_4/Ti_3C_2T_x$, it is quite logical that for the more ordered structure with small crystals of the former, the HER overpotential is lower (45 mV) than for the latter with nanoparticles in the form of amorphous spheres (87 mV).

The major influence of the modifier's crystal structure on catalyst activity can also be seen in the comparison of two $NiFe_2O_4/Ti_3C_2T_x$ catalyst systems. In one case, where $NiFe_2O_4$ was present as parallelly intergrown nanowires (confirmed by TEM and SEM images), the HER overpotential was 584 mV, only slightly better than pristine $Ti_3C_2T_x$ (650 mV), likely due to an insufficient increase in surface area [52]. In the second case – with spinel-structured crystals – the HER overpotential was substantially lower at 173 mV at 10 mA/cm^2 [36]. On the other hand, with a more favorable catalyst morphology, a significant improvement in its characteristics can be achieved. For example, molybdenum oxide with a nanorod structure and a fairly high average diameter of 250 nm (in [52], it was 0.18–5.64 nm), thanks to a chaotically interconnected structure visible in SEM images, demonstrated an HER overpotential of 192 mV even in its pure form. Its combination with MXene allowed this value to be more than halved – to 91 mV [71]. The authors attribute this to an increase in the catalyst's surface area and electrical conductivity.

The modification of 2D MXene materials with various layered inorganic compounds is widespread [41, 72–76]. The orientation of these layered modifiers relative to the flakes of the MXene matrix can vary: they can be arranged either parallel or perpendicular to them. In both cases, an increase in the catalytic activity of the resulting composite is usually observed. However, it is assumed that with parallel arrangement, the main contribution to performance improvement comes from the distribution of modifier particles over the surface of individual MXene layers, which increases their contact area with the electrolyte. In the case of perpendicular orientation, a more effective separation of both the modifier layers and the MXene layers themselves occurs, which should lead to a more significant increase in the total active surface area of the catalyst and, consequently, to a more substantial reduction in the HER overpotential under equal current densities.

For example, in study [72], hexagonal nanoplates of mixed nickel and cobalt oxide were deposited on the surface of MXene flakes by a hydrothermal method. However, even the composite catalyst with the composition $Ni_{0.09}Co_{2.91}O_4/Ti_3C_2T_x$, considered optimal by the authors, showed a relatively high HER overpotential of 210 mV at 10 mA/cm^2. SEM analysis revealed a rather chaotic arrangement of the modifier nanoparticles on the MXene surface, with a predominant parallel orientation, which may indicate the low efficiency of such a morphology.

Layered transition metal hydroxides are also actively used as modifying additives to MXenes. Composites with both single metal hydroxides [73, 74] and mixed layered double hydroxides (LDHs) [75] have been investigated. The $VOOH/Ti_3C_2T_x$ catalyst contained VOOH nanosheets with a diameter of about 600 nm, which, according to SEM images, were primarily anchored on the MXene surface in a horizontal (parallel) position [73]. Despite the absence of a pronounced effect of increasing the active area due to this morphology, the HER overpotential for this material was 100 mV at 10 mA/cm^2, indicating its higher intrinsic catalytic activity compared to the aforementioned $Ni_{0.09}Co_{2.91}O_4/Ti_3C_2T_x$ with a similar morphology. In contrast, a composite catalyst in which cobalt hydroxide nanoplates were anchored perpendicularly to the MXene flakes demonstrated excellent activity [74]. Such a structure provided a significant increase in the modifier's contact area with the electrolyte and allowed the HER overpotential to be reduced to 21 mV, which is almost identical to the value measured in the same study for a platinum catalyst. Excellent results were also shown by the NiFeCo–LDH@$Ti_3C_2T_x$ composite, containing a layered hydroxide of three transition metals, where the HER overpotential was 34 mV [75].

Among other layered additives to MXenes that effectively reduce HER overpotential, cobalt phosphide with the composition Co_2P can be noted, for which a value of 42 mV was achieved. This result correlates well with its calculated Gibbs free energy of hydrogen adsorption (-0.067 eV) [41]. A highly active combination also proved to be MXene and CoBDC nanosheets (a metal-organic framework), where the Co–O–Ti bond formed at the phase interface facilitated improved charge transfer and optimization of the active site's electronic structure. This led to a reduction in ΔG_{H*} to -0.2 eV and the HER overpotential to 29 mV [76].

Modification of MXenes with transition metal sulfides generally leads to a moderate increase in HER catalytic activity. This may be due to both the not remarkably high activity of the sulfide phases used and an insufficient increase in the effective surface area of the catalysts. For example, cobalt sulfide was synthesized on the surface of $Ti_3C_2T_x$ MXene flakes by a hydrothermal method followed by sulfurization. Although transmission electron microscopy showed the formation of CoS_2 particles with a clear crystalline structure in the form of nanowires, SEM data indicated their rather dense arrangement, predominantly parallel to the substrate plane [53]. As a result, the CoS_2@MXene composite showed only a slight reduction in HER overpotential (175 mV at 10 mA/cm^2) compared to the individual components (225 mV for CoS_2 and 260 mV for MXene). Another cobalt sulfide, Co_4S_3, showed a slightly better result of 142 mV, which correlates well with a more uniform distribution of its nanoparticles on the MXene flakes [37]. However, even in this case, according to SEM images, there was no effective separation of MXene flakes, which probably limited further reduction in overpotential. In another study [48], based on hydrogen adsorption energy calculations, it was predicted that V_2CT_x MXene (ΔG_{H*} = 0.38 eV) should have better catalytic activity than $Ti_3C_2T_x$ (ΔG_{H*} = 0.46 eV). Both these materials were modified with nickel sulfide (NiS_2), which uniformly and densely coated their surfaces in the form of spherical nanoparticles. Electrochemical tests confirmed the prediction: on NiS_2/V-MXene, the HER overpotential was 179 mV, slightly lower than on NiS_2/Ti-MXene (205 mV). The highest overpotential among MXenes modified with sulfides (196 mV) was recorded for the $Ni_{0.9}Fe_{0.1}PS_3$@$Ti_3C_2T_x$ composite [54]. Such low activity can be explained by the arrangement of the modifier nanoparticles, which have a mosaic structure, parallel to the surface of the MXene flakes, which did not contribute to an increase in the material's total contact area with the electrolyte.

Non-metallic compounds, particularly carbon nanotubes (CNTs), are also used in composite catalysts with MXenes. Depending on their diameter and integration method, CNTs can perform various functions: either serving as a protective framework for MXene flakes, preventing their aggregation [47], or physically separating MXene layers by being positioned perpendicularly between them, thereby increasing the accessible surface area [25, 26].

In the first case, described in study [47], hexagonal MoN MXene nanoparticles (3–5 nm in size) were anchored on the inner walls of boron and nitrogen-doped carbon nanotubes (BCN-CNTs) with a diameter of 30–50 nm. Both components (BCN-CNTs and MoN) were presumed to contribute to catalysis. The resulting catalyst exhibited an HER overpotential of 118 mV at 10 mA/cm^2. This moderate activity could be attributed to either insufficiently high intrinsic catalytic activity of the components or to hindered electrolyte diffusion into the nanotubes, which limited access to the more active MoN component. Indeed, the calculated Gibbs free energy of hydrogen adsorption for MoN (-0.78 eV) was more than twice as close to the optimal zero value than that for BCN-CNTs (-1.90 eV).

A significantly better increase in surface area is achieved when CNTs are grown directly between MXene layers. The activity of such composite catalysts strongly depends on the composition of the MXene used. As previously mentioned [48], V_2CT_x MXene possesses higher intrinsic catalytic activity compared to $Ti_3C_2T_x$. This was confirmed in study [25], where an overpotential of only 27 mV at

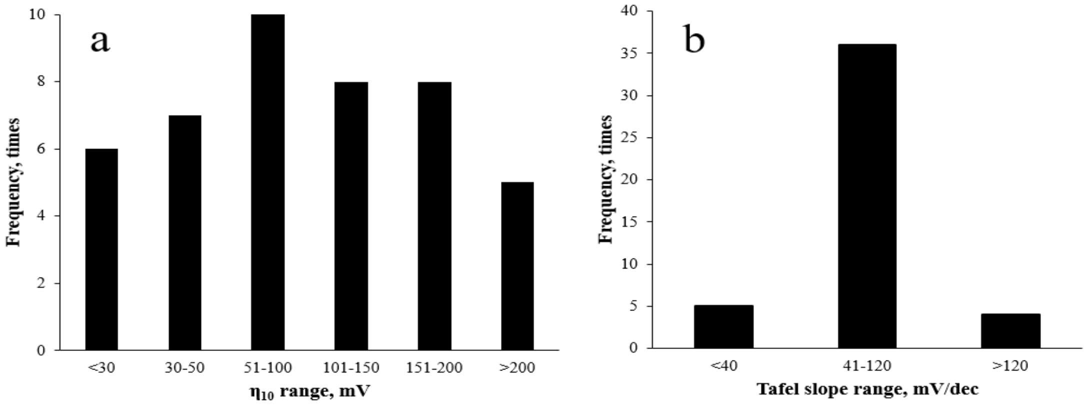

Fig. 8. Distribution of HER overpotentials (a) and Tafel slopes (b) for the reviewed catalysts across value ranges.

10 mA/cm^2 was obtained for the MWCNT@V_2CT_x catalyst (multi-walled CNTs on V_2CT_x). Meanwhile, for the 3D CNTs@$Ti_3C_2T_x$ composite (a three-dimensional structure of CNTs on $Ti_3C_2T_x$), this value was 93 mV at the same current density [26].

Since the catalytic properties of the materials discussed in this review vary widely, their HER overpotentials (η_{10}) and Tafel slope values were compiled and presented graphically (Fig. 8) for a more visual comparison of their efficiencies. Analysis of the overpotential distribution (Fig. 8a) shows a pattern close to a normal distribution, with the maximum frequency occurring in the 51 to 100 mV range. This indicates a good average activity of catalysts being developed in this research area. The Tafel slope values (Fig. 8b) were grouped according to the predominant HER mechanism: below 40 mV/dec (Tafel rate-limiting step), from 40 to 120 mV/dec (Heyrovsky rate-limiting step), and around 120 mV/dec (Volmer rate-limiting step) [30]. It should be noted, however, that Tafel slope values significantly exceeding 120 mV/dec are most likely the result of an erroneous determination of this parameter. The histogram presented in Fig. 8b clearly shows that, for most the systems investigated, the second HER step is predominantly the Heyrovsky step.

Additionally, for a comparative analysis of Gibbs free energies, their values were presented as a diagram showing the respective deviations from the ideal value (0 eV) for each catalyst (Fig. 9). The materials exhibiting the best activity according to this parameter were $Pt_{3.21}Ni/Ti_3C_2T_x$ [63] (-0.03 eV), CoP/Mo_2CT_x [65] (-0.037 eV), and graphene-coated $Co_{0.31}Mo_{1.69}C$ [68] (0.05 eV).

5. Conclusion

Hydrogen represents an environmentally friendly alternative to fossil fuels and has the potential to meet growing global energy demands. Water electrolysis is the "greenest" method for its production; however, to enhance the economic efficiency of this

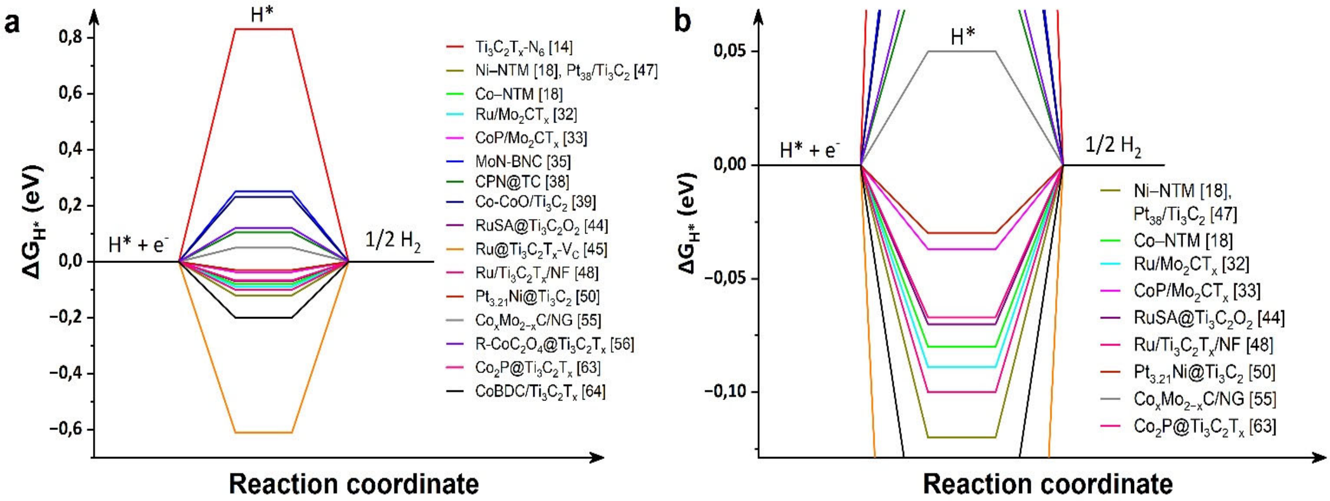

Fig. 9. Gibbs free energies of the reviewed catalysts: general view (a) and enlarged view (b).

process, catalysis of the hydrogen evolution reaction is necessary to reduce energy consumption.

Noble metals are traditionally considered the most effective HER catalysts, but their high cost severely limits their widespread industrial application. Among catalysts based on more accessible transition metals, some active options exist, but their common problem is low specific surface area due to nanoparticle aggregation. In this context, layered materials of the MXene class offer an excellent platform (matrix) for creating composite catalysts due to their unique combination of high electrical conductivity, good chemical and mechanical stability, as well as an inherently developed surface and capacity for functionalization. The analysis of the reviewed studies shows that the best catalytic performance among MXene-based composite materials is demonstrated by systems incorporating noble metal atoms or nanoparticles, various morphologies of cobalt phosphides, layered transition metal hydroxides, certain metal-organic frameworks, and carbon nanotubes integrated into the MXene structure.

This review aimed to summarize and compare data on various materials investigated as MXene-based HER catalysts. However, it must be noted that in many published studies, the conditions for electrochemical tests vary significantly, and the data provided are not always complete, which complicates direct and accurate comparison of results. Moreover, long-term stability tests of catalysts are very rarely conducted until a significant degradation of measured parameters or for a sufficiently long duration, making it impractical to compare stability results obtained with different testing times, even if other conditions were identical. Due to these complexities, a detailed analysis of catalyst stability was not included within the scope of this review. To address these issues and enable adequate comparison of developing catalytic systems, there is an urgent need for the standardization of electrochemical measurement conditions, particularly concerning the selection of standard current densities for overpotential assessment and the definition of regulated minimum durations for stability tests.

6. Future perspectives and challenges

Despite significant achievements in the development of MXene-based HER catalysts, several opportunities remain unexplored and unresolved problems persist:

1. Although theoretical calculations indicate many potentially more catalytically active MXene compounds, most studies use the almost inactive Ti_3C_2 due to its relative ease of synthesis. To achieve greater activity of the resulting composite catalysts, it is necessary to use more active MXenes from the outset, but this requires the development of energy- and cost-effective methods for their synthesis.

2. During the literature search on this topic, only a few attempts were found to control surface groups using both top-down and bottom-up methods, while modelling studies indicate that MXenes with functional groups of the same type are the most catalytically active in terms of HER. Therefore, this direction needs to be developed in practice.

3. In most of the studies reviewed, MXene mixed with additives is applied to a substrate (e.g., nickel foam) or mixed with a binder (PVdF). However, thanks to the layered structure of the MXene suspension, it is possible to obtain self-standing electrodes by filtration without the use of additional materials, which can reduce its cost and weight, allowing for more efficient use of the electrolyser space, which is beneficial for industrial applications. At the same time, the question of mechanical stability remains open, which can be solved by improving the design of the electrolyser and by carefully controlling the composition and conditions of electrode production.

4. MXenes are subject to oxidation and structural degradation during prolonged electrolysis, especially in aqueous environments. This requires improving their chemical stability and applying protective solutions that would maintain their activity in acidic and alkaline conditions. Improving stability is a key condition for their practical use.

5. Comparing the results of different studies is difficult due to differences in test conditions and incomplete data. For an objective assessment, it is necessary to introduce uniform standards for measuring overvoltage and compare it with the calculated values of ΔG_{H^*}, as well as use in situ methods to monitor activity and degradation in real time.

6. Despite success in laboratory conditions, there is still insufficient data on the use of MXene in practical electrolysers. Promising tasks include the creation of stable and mechanically strong electrodes, the development of full-fledged HER/OER systems, and conducting long-term tests under real-world conditions.

Acknowledgments

This research is funded by the Ministry of Science and Higher Education of the Republic of Kazakhstan (Grant No. BR21882200).

References

[1]. M. Filonchyk, M.P. Peterson, H. Yan, et al., Greenhouse gas emissions and reduction strategies for the world's largest greenhouse gas emitters, *Sci. Total Environ.* 944 (2024) 173895. DOI: 10.1016/j.scitotenv.2024.173895

[2]. J. Incer-Valverde, A. Korayem, G. Tsatsaronis, T. Morosuk, “Colors” of hydrogen: Definitions and carbon intensity, *Energy Convers. Manag.* 291 (2023) 117294. DOI: 10.1016/j.enconman.2023.117294

[3]. Y. Shi, S. Xiao, S. Jiao, et al., Hydrogen evolution electrodes: Materials and mechanisms in alkaline electrolysis, *Desalination* 586 (2024) 117887. DOI: 10.1016/j.desal.2024.117887

[4]. W. Sheng, M. Myint, J.G. Chen, Y. Yan, Correlating the hydrogen evolution reaction activity in alkaline electrolytes with the hydrogen binding energy on monometallic surfaces, *Energy Environ. Sci.* 6 (2013) 1509–1512. DOI: 10.1039/c3ee00045a

[5]. J. Mahmood, F. Li, S.M. Jung, et al., An efficient and pH-universal ruthenium-based catalyst for the hydrogen evolution reaction, *Nat. Nanotechnol.* 12 (2017) 441–446. DOI: 10.1038/nnano.2016.304

[6]. A. Oh, Y.J. Sa, H. Hwang, et al., Rational design of Pt–Ni–Co ternary alloy nanoframe crystals as highly efficient catalysts toward the alkaline hydrogen evolution reaction, *Nanoscale* 8 (2016) 16379–16386. DOI: 10.1039/c6nr04572c

[7]. J. Zhang, T. Wang, P. Liu, et al., Efficient hydrogen production on MoNi4 electrocatalysts with fast water dissociation kinetics, *Nat. Commun.* 8 (2017) 15437. DOI: 10.1038/ncomms15437

[8]. A.I. Inamdar, H.S. Chavan, B. Hou, et al., A Robust Nonprecious CuFe Composite as a Highly Efficient Bifunctional Catalyst for Overall Electrochemical Water Splitting, *Small* 16 (2020). DOI: 10.1002/smll.201905884

[9]. Y. Ha, L. Shi, X. Yan, et al., Multifunctional Electrocatalysis on a Porous N-Doped $NiCo_2O_4$@C Nanonetwork, *ACS Appl. Mater. Interfaces* 11 (2019) 45546–45553. DOI: 10.1021/acsami.9b13580

[10]. Y. Li, H. Zhang, M. Jiang, et al., 3D Self-Supported Fe-Doped Ni2P Nanosheet Arrays as Bifunctional Catalysts for Overall Water Splitting, *Adv. Funct. Mater.* 27 (2017) 1–8. DOI: 10.1002/adfm.201702513

[11]. J. Lai, S. Li, F. Wu, et al., Unprecedented metal-free 3D porous carbonaceous electrodes for full water splitting, *Energy Environ. Sci.* 9 (2016) 1210–1214. DOI: 10.1039/C5EE02996A

[12]. K. Qu, Y. Zheng, Y. Jiao, et al., Polydopamine-Inspired, Dual Heteroatom-Doped Carbon Nanotubes for Highly Efficient Overall Water Splitting, *Adv. Energy Mater.* 7 (2017). DOI: 10.1002/aenm.201602068

[13]. Z. Peng, S. Yang, D. Jia, et al., Homologous metal-free electrocatalysts grown on three-dimensional carbon networks for overall water splitting in acidic and alkaline media, *J. Mater. Chem. A* 4 (2016) 12878–12883. DOI: 10.1039/c6ta04426c

[14]. Z.W. Seh, J. Kibsgaard, C.F. Dickens,et al., Combining theory and experiment in electrocatalysis: Insights into materials design, *Science* 355 (6321) 2017. DOI: 10.1126/science.aad4998

[15]. M. Ryabicheva, Y. Zhigalenok, S. Abdimomyn, et al., From lab to market: Economic viability of modern hydrogen evolution reaction catalysts, *Fuel* 395 (2025) 135227. DOI: 10.1016/j.fuel.2025.135227

[16]. F. Du, Y. Zhang, H. He, et al., Electrodeposited amorphous cobalt phosphosulfide on Ni foams for highly efficient overall water splitting, *J. Power Sources* 431 (2019) 182–188. DOI: 10.1016/j.jpowsour.2019.05.063

[17]. C. Ma, L. Sang, X. Duan, et al., An efficient method for enhancing adhesion and uniformity of Al2O3 coatings on nickel micro-foam used in micropacked beds, *Chin. J. Chem.* 39 (2021) 162–172. DOI: 10.1016/j.cjche.2021.05.022

[18]. X. Chen, X. Zhai, J. Hou, et al., Tunable nitrogen-doped delaminated 2D MXene obtained by NH_3/Ar plasma treatment as highly efficient hydrogen and oxygen evolution reaction electrocatalyst, *Chem. Eng. J.* 420 (2021) 129832. DOI: 10.1016/j.cej.2021.129832

[19]. S.Y. Pang, W.F. Io, L.W. Wong, et al., Efficient Energy Conversion and Storage Based on Robust Fluoride-Free Self-Assembled 1D Niobium Carbide in 3D Nanowire Network, *Adv. Sci.* 7 (2020) 1–8. DOI: 10.1002/advs.201903680

[20]. S.Y. Pang, W.F. Io, J. Hao, Facile Atomic-Level Tuning of Reactive Metal–Support Interactions in the Pt QDs@ HF-Free MXene Heterostructure for Accelerating pH-Universal Hydrogen Evolution Reaction, *Adv. Sci.* 8 (2021) 1–9. DOI: 10.1002/advs.202102207

[21]. R. Ali, M. Islam, M. Shafi, et al., Developments and prospects of MXenes for energy storage and environmental sustainability, *Coord. Chem. Rev.* 540 (2025) 216797. DOI: 10.1016/j.ccr.2025.216797

[22]. A. Baimenov, C. Daulbayev, S.G. Poulopoulos, V.N. Mochalin, MXene filled hydrogel and aerogel

composites, *Mater. Today* 78 (2024) 75–91. DOI: 10.1016/j.mattod.2024.06.011

[23]. X. Liu, M. Albloushi, M. Galvin, et al., A paired alkaline electrolyzer for furfural oxidation and hydrogen evolution over noble metal-free NiFe/Ni and Co/MXene catalysts, *Green Chem.* 2024. DOI: 10.1039/d4gc04447a

[24]. C.F. Du, X. Sun, H. Yu, et al., Synergy of Nb Doping and Surface Alloy Enhanced on Water–Alkali Electrocatalytic Hydrogen Generation Performance in Ti-Based MXene, *Adv. Sci.* 6 (2019) 1–7. DOI: 10.1002/advs.201900116

[25]. S.A. Zahra, S. Rizwan, MWCNT-modified MXene as cost-effective efficient bifunctional catalyst for overall water splitting, *RSC Adv.* 12 (2022) 8405–8413. DOI: 10.1039/d2ra00868h

[26]. X. Wang, S. Wang, J. Qin, et al., Constructing Conductive Bridge Arrays between $Ti_3C_2T_x$ MXene Nanosheets for High-Performance Lithium-Ion Batteries and Highly Efficient Hydrogen Evolution, *Inorg. Chem.* 58 (2019) 16524–16536. DOI: 10.1021/acs.inorgchem.9b02513

[27]. T.A. Le, N.Q. Tran, Y. Hong, et al., Porosity-Engineering of MXene as a Support Material for a Highly Efficient Electrocatalyst toward Overall Water Splitting, *ChemSusChem* 13 (2020) 945–955. DOI: 10.1002/cssc.201903222

[28]. S.G. Peera, R. Koutavarapu, L. Chao, et al., 2D MXene Nanomaterials as Electrocatalysts for Hydrogen Evolution Reaction (HER): A Review, *Micromachines* 13 (2022) 1499. DOI: 10.3390/mi13091499

[29]. H. Ooka, J. Huang, K.S. Exner, The Sabatier Principle in Electrocatalysis: Basics, Limitations, and Extensions, *Front. Energy Storage* 9 (2021). DOI: 10.3389/fenrg.2021.654460

[30]. I.H. Sajid, M.Z. Iqbal, S. Rizwan, Recent advances in the role of MXene based hybrid architectures as electrocatalysts for water splitting, *RSC Adv.* 14 (2024) 6823–6847. DOI: 10.1039/D3RA06725D

[31]. M. Kaleem Shabbir, F. Arif, H. Asghar, et al., Two-Dimensional MXene-Based Electrocatalysts: Challenges and Opportunities, *Chem. Rec.* 24 (2024). DOI: 10.1002/tcr.202400047

[32]. A. Zamhuri, G.P. Lim, N.L. Ma, et al., MXene in the lens of biomedical engineering: synthesis, applications and future outlook, *BioMed. Eng. OnLine* 20 (2021) 33. DOI: 10.1186/s12938-021-00873-9

[33]. L. Yuan, S. Liu, S. Xu, et al., Modulation of Volmer step for efficient alkaline water splitting implemented by titanium oxide promoting surface reconstruction of cobalt carbonate hydroxide, *Nano Energy* 82 (2020) 105732. DOI: 10.1016/j.nanoen.2020.105732

[34]. L.P. Hao, A. Hanan, R. Walvekar, et al., Synergistic Integration of MXene and Metal-Organic Frameworks for Enhanced Electrocatalytic Hydrogen Evolution in an Alkaline Environment, *Catalysts* 13 (2023) 1–13. DOI: 10.3390/catal13050802

[35]. G.T.M. Kadja, S.A.C. Natalya, F. Balqis, et al., Gold nanoparticles–supported Ti_3C_2 MXene nanosheets for enhanced electrocatalytic hydrogen evolution reaction, *Nano-Struct. Nano-Objects.* 36 (2023) 101059. DOI: 10.1016/j.nanoso.2023.101059

[36]. P.V. Shinde, P. Mane, B. Chakraborty, C. Sekhar Rout, Spinel $NiFe_2O_4$ nanoparticles decorated 2D Ti_3C_2 MXene sheets for efficient water splitting: Experiments and theories, *J. Colloid Interface Sci.* 602 (2021) 232–241. DOI: 10.1016/j.jcis.2021.06.007

[37]. M. Kumar, B. Ramulu, J.S. Yu, MXene composite with Ni/Co sulfide for enhanced hydrogen evolution reaction, *Mater. Chem. Front.* 8 (2024) 1844–1851. DOI: 10.1039/d4qm00095a

[38]. Y. Qian, K. Zhang, L.W. Tan, et al., Highly reversible and safe lithium metal batteries enabled by Non-flammable All-fluorinated carbonate electrolyte conjugated with 3D flexible MXene-based lithium anode, *Chem. Eng. J.* 440 (2021) 135818. DOI: 10.1016/j.cej.2022.135818

[39]. E. Uwadiunor, V. Kotasthane, D.K. Yesudoss, et al., Pt-like catalytic activity from an atomistically engineered carbonitride MXene for sustainable hydrogen production, *Chem Catalysis* 3 (2023) 100634. DOI: 10.1016/j.checat.2023.100634

[40]. Y. Wu, L. Wang, T. Bo, et al., Boosting Hydrogen Evolution in Neutral Medium by Accelerating Water Dissociation with Ru Clusters Loaded on Mo_2CT_x MXene, *Adv. Funct. Mater.* 33 (2023) 1–7. DOI: 10.1002/adfm.202214375

[41]. Z. Lv, W. Ma, J. Dang, et al., Induction of Co_2P Growth on a MXene ($Ti_3C_2T_x$)-Modified Self-Supporting Electrode for Efficient Overall Water Splitting, *J. Phys. Chem. Lett.* 12 (2021) 4841–4848. DOI: 10.1021/acs.jpclett.1c01345

[42]. M. Pandey, K.S. Thygesen, Two-Dimensional MXenes as Catalysts for Electrochemical Hydrogen Evolution: A Computational Screening Study, *J. Phys. Chem. C* 121 (2017) 13593–13598. DOI: 10.1021/acs.jpcc.7b05270

[43]. S. Ma, X. Fan, Y. An, et al., Exploring the catalytic activity of MXenes $M_{n+1}CnO_2$ for hydrogen evolution, *J. Mater. Sci.* 54 (2019) 11378–11389. DOI: 10.1007/s10853-019-03712-4

[44]. A.D. Handoko, K.D. Fredrickson, B. Anasori, et al., Tuning the Basal Plane Functionalization of Two-Dimensional Metal Carbides (MXenes) To Control Hydrogen Evolution Activity, *ACS Appl. Energy Mater.* 1 (2018) 173–180. DOI: 10.1021/acsaem.7b00054

[45]. Y. Tan, Z. Zhu, X. Zhang, et al., $Nb_4C_3T_x$ (MXene) as a new stable catalyst for the hydrogen evolution reaction, *J. Hydrogen Energy* 46 (2021) 1955–1966. DOI: 10.1016/j.ijhydene.2020.10.046

[46]. H. Zong, R. Qi, K. Yu, Z. Zhu, Ultrathin Ti_2NT_x MXene-wrapped MOF-derived CoP frameworks towards hydrogen evolution and water oxidation, *Electrochim. Acta* 393 (2021). DOI: 10.1016/j.electacta.2021.139068

[47]. J. Miao, Z. Lang, X. Zhang, et al., Polyoxometalate-Derived Hexagonal Molybdenum Nitrides (MXenes) Supported by Boron, Nitrogen Codoped Carbon Nanotubes for Efficient Electrochemical Hydrogen Evolution from Seawater, *Adv. Funct. Mater.* 29 (2019) 1–9. DOI: 10.1002/adfm.201805893

[48]. P. Kuang, M. He, B. Zhu, et al., 0D/2D NiS_2/V-MXene composite for electrocatalytic H_2 evolution, *J. Catal.* 375 (2019) 8–20. DOI: 10.1016/j.jcat.2019.05.019

[49]. L. Meng, L.K. Yan, F. Viñes, F. Illas, Effect of terminations on the hydrogen evolution reaction mechanism on Ti_3C_2 MXene, *J. Mater. Chem. A* 11 (2023) 6886–6900. DOI: 10.1039/d3ta00261f

[50]. Z. Lv, W. Ma, M. Wang, et al., Co-Constructing Interfaces of Multiheterostructure on MXene ($Ti_3C_2T_x$)-Modified 3D Self-Supporting Electrode for Ultraefficient Electrocatalytic HER in Alkaline Media, *Adv. Funct. Mater.* 31 (2021) 2102576. DOI: 10.1002/adfm.202102576

[51]. D. Guo, X. Li, Y. Jiao, et al., A dual-active Co-CoO heterojunction coupled with Ti_3C_2-MXene for highly-performance overall water splitting, *Nano Res.* 15 (2022) 238–247. DOI: 10.1007/s12274-021-3465-1

[52]. M. Khalil, M. Lesa, A.G. Juandito, et al., A SBA-15-templated mesoporous $NiFe_2O_4$/MXene nanocomposite for the alkaline hydrogen evolution reaction, *Mater. Adv.* 4 (2023) 3853–3862. DOI: 10.1039/d3ma00289f

[53]. S. Han, Y. Chen, Y. Hao, et al., Multi-dimensional hierarchical CoS_2@MXene as trifunctional electrocatalysts for zinc-air batteries and overall water splitting, *Sci. China Mater.* 64 (2021) 1127–1138. DOI: 10.1007/s40843-020-1524-5

[54]. C. Du, K.N. Dinh, Q. Liang, et al., Self-Assemble and In Situ Formation of Ni1−xFexPS3 Nanomosaic-Decorated MXene Hybrids for Overall Water Splitting, *Adv. Energy Mater.* 8 (2018) 1801127. DOI: 10.1002/aenm.201801127

[55]. T. Wu, X. Pang, S. Zhao, et al., One-Step Construction of Ordered Sulfur-Terminated Tantalum Carbide MXene for Efficient Overall Water Splitting, *Small Structures* 3 (2022) 1–7. DOI: 10.1002/sstr.202100206

[56]. C. Daulbayev, A. Nursharip, Z. Tauanov, et al., Mechanisms of mercury removal from water with highly efficient MXene and silver-modified polyethyleneimine cryogel composite filters, *Adv. Compos. Hybrid Mater.* 7 (2024) 139. DOI: 10.1007/s42114-024-00945-z

[57]. Y. Zou, S.A. Kazemi, G. Shi,et al., Ruthenium single-atom modulated $Ti_3C_2T_x$ MXene for efficient alkaline electrocatalytic hydrogen production, *EcoMat* 5 (2023) 1–13. DOI: 10.1002/eom2.12274

[58]. X. Wang, J. Ding, W. Song, et al., Cation Vacancy Clusters in $Ti_3C_2T_x$ MXene Induce Ultra-Strong Interaction with Noble Metal Clusters for Efficient Electrocatalytic Hydrogen Evolution, *Adv. Energy Mater.* 13 (2023) 1–11. DOI: 10.1002/aenm.202300148

[59]. K. Gothandapani, G. Tamil Selvi, R. Sofia Jennifer, et al., Ni-Ti_3C_2 MXene composite derived from Ni-metal organic framework for electrochemical hydrogen evolution reaction in acidic and alkaline medium International, *J. Hydrogen Energy* 52 (2024) 1164–1171. DOI: 10.1016/j.ijhydene.2023.10.022

[60]. L. Xiu, W. Pei, S. Zhou, et al., Multilevel Hollow MXene Tailored Low-Pt Catalyst for Efficient Hydrogen Evolution in Full-pH Range and Seawater, *Adv. Funct. Mater.* 30 (2020) 1–10. DOI: 10.1002/adfm.201910028

[61]. A. Kong, M. Peng, H. Gu, et al., Synergetic control of Ru/MXene 3D electrode with superhydrophilicity and superaerophobicity for overall water splitting, *Chem. Eng. J.* 426 (2021). DOI: 10.1016/j.cej.2021.131234

[62]. R. Luo, R. Li, C. Jiang, et al., Facile synthesis of cobalt modified 2D titanium carbide with enhanced hydrogen evolution performance in alkaline media, International, *J. Hydrogen Energy* 46 (2021) 32536–32545. DOI: 10.1016/j.ijhydene.2021.07.110

[63]. Y. Jiang, X. Wu, Y. Yan, et al., Coupling PtNi Ultrathin Nanowires with MXenes for Boosting Electrocatalytic Hydrogen Evolution in Both Acidic and Alkaline Solutions, *Small* 15 (2019) 1–9. DOI: 10.1002/smll.201805474

[64]. L. Xiu, Z. Wang, M. Yu, et al., Aggregation-

Resistant 3D MXene-Based Architecture as Efficient Bifunctional Electrocatalyst for Overall Water Splitting, *ACS Nano* 12 (2018) 8017–8028. DOI: 10.1021/acsnano.8b02849

[65]. S. Liu, Z. Lin, R. Wan, et al., Cobalt phosphide supported by two-dimensional molybdenum carbide (MXene) for the hydrogen evolution reaction, oxygen evolution reaction, and overall water splitting, *J. Mater. Chem. A* 9 (2021) 21259–21269. DOI: 10.1039/d1ta05648d

[66]. K. Yu, J. Zhang, Y. Hu, et al., Ni Doped Co-MOF-74 Synergized with 2D $Ti_3C_2T_x$ MXene as an Efficient Electrocatalyst for Overall Water-Splitting, *Catalysts* 14 (2024) 184. DOI: 10.3390/catal14030184

[67]. Y. Tang, C. Yang, M. Sheng, et al., Phosphorus-doped molybdenum carbide/MXene hybrid architectures for upgraded hydrogen evolution reaction performance over a wide pH range, *Chem. Eng. J.* 423 (2021) 130183. DOI: 10.1016/j.cej.2021.130183

[68]. X. Wu, S. Zhou, Z. Wang, et al., Engineering Multifunctional Collaborative Catalytic Interface Enabling Efficient Hydrogen Evolution in All pH Range and Seawater, *Adv. Energy Mater.* 9 (2019) 1–11. DOI: 10.1002/aenm.201901333

[69]. L. Wang, Y. Hao, L. Deng, et al., Rapid complete reconfiguration induced actual active species for industrial hydrogen evolution reaction, *Nat. Commun.* 13 (2022). DOI: 10.1038/s41467-022-33590-5

[70]. W. Guo, B. Wang, Q. Shu, An Efficient and Stable MXene-Immobilized, Cobalt-Based Catalyst for Hydrogen Evolution Reaction, *Metals* 14 (2024). DOI: 10.3390/met14080922

[71]. I. Ashraf, S. Ahmad, S. Rizwan, M. Iqbal, Fabrication of $Ti_3C_2@MoO_3$ nanocomposite as an electrode material for highly efficient and durable water splitting system, *Fuel* 299 (2021) 120928. DOI: 10.1016/j.fuel.2021.120928

[72]. P. Xu, H. Wang, J. Liu, et al., High-Performance $Ni_xCo_{3-x}O_4/Ti_3C_2T_x$-HT Interfacial Nanohybrid for Electrochemical Overall Water Splitting, *ACS Appl. Mater. Interfaces* 13 (2021) 34308–34319. DOI: 10.1021/acsami.1c08032

[73]. L. Yan, X. Chen, X. Liu, et al., In situ formed VOOH nanosheet arrays anchored on a $Ti_3C_2T_x$ MXene as a highly efficient and robust synergistic electrocatalyst for boosting water oxidation and reduction, *J. Mater. Chem. A* 8 (2020) 23637–23644. DOI: 10.1039/D0TA09410B

[74]. L. Li, D. Yu, P. Li, et al., Interfacial electronic coupling of ultrathin transition-metal hydroxide nanosheets with layered MXenes as a new prototype for platinum-like hydrogen evolution, *Energy Environ. Sci.* 14 (2021) 6419–6427. DOI: 10.1039/D1EE02538D

[75]. S. Hussain, D. Vikraman, G. Nazir, et al., Development of Binder-Free Three-Dimensional Honeycomb-like Porous Ternary Layered Double Hydroxide-Embedded MXene Sheets for Bi-Functional Overall Water Splitting Reactions, *Nanomaterials* 12 (2022). DOI: 10.3390/nano12162886

[76]. L. Wang, L. Song, Z. Yang, et al., Electronic Modulation of Metal–Organic Frameworks by Interfacial Bridging for Efficient pH-Universal Hydrogen Evolution, Adv. Funct. Mater. 33 (2023) 1–10. DOI: 10.1002/adfm.202210322